NOVEL RECONSTRUCTION WITH INTER-FRAME MOTION COMPENSATION FOR FAST SUPER-RESOLUTION LIVE CELL IMAGING

Adam Harmanec[1,2] *Zuzana Kadlecova*[2,3] *Filip Sroubek*[1]

[1]Institute of Information Theory and Automation, Czech Academy of Sciences, Prague, CZ
[2]Department of Histology and Embryology, Faculty of Medicine, Masaryk University, Brno, CZ
[3]Cambridge Institute for Medical Research, University of Cambridge, Cambridge, UK

2022 IEEE International Conference on Image Processing (ICIP) | 978-1-6654-9620-9/22/$31.00 ©2022 IEEE | DOI: 10.1109/ICIP46576.2022.9897635

ABSTRACT

Structured illumination microscopy is a widely popular super-resolution technique for live cell imaging capable of surpassing the diffraction limit. Its temporal resolution is limited by the need to capture multiple low-resolution images to reconstruct a single high-resolution image. When observing rapid biological processes, the local movement between frames leads to the formation of reconstruction artifacts, which subsequently impair the data interpretation. We propose to include this type of movement in the definition of the image formation forward problem. The motion can then be estimated from the original data using optical flow, and the optimization problem is solved using the alternating direction method of multipliers. Our approach is tested against other reconstruction techniques on both synthetic and real biological data.

Index Terms— Image reconstruction, structured illumination microscopy (SIM), ADMM, optical flow

1. INTRODUCTION

It has been long understood that the lateral resolution of an optical microscope is bounded by the diffraction limit [1]. Traditional super-resolution methods in image processing [2] exploit the aliasing effect in images with sub-pixel shift to recover corrupted high frequencies, yet the diffraction limit remains unchallenged. On the other hand, microscopy super-resolution methods that have been developed in the last two decades overcome this limitation [3, 4, 5]; however, only structured illumination microscopy (SIM) [4], especially when combined with total illumination reflective fluorescence (TIRF) [6, 7], offers the high temporal and spatial resolution to capture dynamic biological processes in living cells [8]. It uses structured light to increase resolution and conversely assumes that the images are without sub-pixel shift. Our approach described below is suitable for any SIM system, but this work will demonstrate it in a more demanding situation on our custom-built eTIRF-SIM with a 90nm lateral resolution and a temporal resolution of 100-200ms per channel and frame.

Even though this configuration allows rapid imaging, SIM suffers from several inherent limitations. Since multiple consecutive images need to be acquired and reconstructed into a single image with higher resolution, the most dynamic sub-cellular structures appear as artefacts during reconstruction [9] (See the second column of Fig. 5 (a)). Combined with a somewhat low(er) signal-to-noise ratio (SNR) of the individual images, this severely limits the interpretation and quantitative analysis of SIM time-lapse movies. The current research is focused on shortening the acquisition time [8], which, however, results in a further reduction of the SNR.

To address the poor reconstruction fidelity of dynamic sub-cellular features, we propose a method for compensating the local inter-frame movement in the imaging model, therefore radically reducing the number of motion artifacts. In addition, our method is defined in an optimization framework that enables various regularization methods, which can further improve the reconstruction.

This method is practical for several reasons. It allows for a more robust interpretation due to higher data fidelity. It can also be applied to acquiring longer time-lapse movies, where SNR steadily decreases.

2. METHOD

2.1. Forward problem

Similarly to [10, 11] and as visualized in Fig. 1, we define the SIM images formation model as:

$$g = DHIu,$$

where $g = [g_1, ..., g_n]^T$ is a set of the n observed low resolution images, u is the single unknown original high resolution image and D, H and $I = [I_1, ..., I_n]^T$ are the down-sampling, convolution and illumination operators, respectively. The images are column-wise concatenated and all of the operators are linear and represented by matrix multiplication.

The work on this paper was supported by the Czech Science Foundation grant 21-16786M, the Technology Agency of the Czech Republic grant TN01000024 and the SVV project number 260 575.

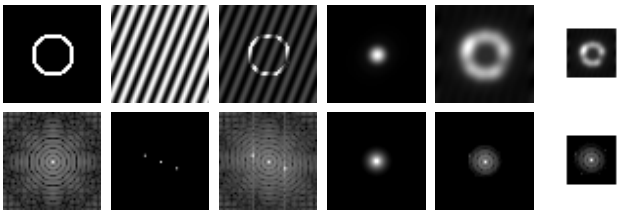

(a) (b) (c) (d) (e) (f)

Fig. 1: Visualisation of the SIM image formation. Images in the top row are in the image domain and images in the bottom row are their Fourier domain counterparts. Image **(a)** is the high-resolution image u (the same in the synthetic data experiments), **(b)** is one of the illumination patterns i_k, **(c)** is the result of $I_k u$, **(d)** are the PSF and OTF, **(e)** is the result of $HI_k u$ and **(f)** one of the final observed images $g_k = DHI_k u$.

The illumination operator I_k corresponds to a pixel-wise multiplication with a structured illumination pattern. Although there are other illumination strategies [12, 13] for which our definition would also work, for simplicity, we will assume the standard two-dimensional sinusoidal pattern created by the inference of two laser beams [4]. The intensity of the k-th pattern at point r_{xy} is a sum of three simple harmonics:

$$i_k(r_{xy}) = \sum_{m=-1}^{1} e^{im(2\pi p_k \cdot r_{xy} + \sigma_k)},$$

where p_k and σ_k are the modulation vector and phase offset respectively. This pattern is chosen deliberately so that its Fourier transform is just three delta function peaks at $\delta(\pm m p_k)$. Intuitively, convolution with these peaks in Fourier space shifts frequencies beyond the diffraction limit closer to the origin and into the support of the optical transfer function (OTF). To separate the three summed components corresponding to each peak, three different images are acquired, each with a different illumination phase σ_k. To achieve good resolution in all directions, three modulation vectors p_k evenly spaced over a circle are usually used, which results in nine ($n = 9$) images in total.

The convolution operator H represents the point-spread function (PSF, i.e. the real space equivalent of the OTF) of the optical system. This operator defines resolution properties of the microscope and acts as a low-pass filter removing high frequency details.

Finally, the down-sampling operator D reduces the lateral resolution by a factor of two in both the horizontal and vertical directions. This represents the sampling frequency of the microscope sensor. In theory, the factor could be lower, since SIM results in just over two-fold resolution gain. This is however not used in practice because less photons would illuminate each pixel and therefore increase noise.

2.2. Proposed extension

The model described above assumes that the unknown image u remains stationary throughout the acquisition of the 9 images. However, each of these 9 images can take between a few tens of milliseconds up to a second or more to acquire, hence this is often not the case. Each of the lower resolution images in the set then effectively corresponds to a different higher resolution image, and this discrepancy inevitably leads to reconstruction artifacts.

To compensate for this, we propose to extend the imaging model with a warping operator $W = [W_1, ..., W_n]$:

$$g = DHIWu$$

One of the images is selected as the reference, e.g. the middle one ($k = 5$), and the W_k operator models the local transformations between the reference and the k-th image. This is done pixel-wise with sub-pixel accuracy.

More formally, each pixel in the transformed image is filled with the value of a pixel in the original image. If the coordinates in the original image are not an integer, the value is interpolated from the nearest neighboring pixels.

2.3. Finding a solution

Here we seek to find the original sharp image u that best explains (*in the least squares sense*) the measured data g. That alone would not be stable and so we also incorporate a regularization factor. We are using total variation (TV) [14] but other methods could also be used. This results in the following optimization task:

$$u = \arg\min_u \frac{1}{2}||DHIWu - g||_2^2 + \gamma||\nabla u||_1$$

The L_1 norm (and other forms of regularization) are generally non-smooth. We can however use the popular optimization framework alternating direction method of multipliers (ADMM) [15] that splits the objective into several simpler problems.

First, we need to isolate the L_1 term to only contain a single variable. This can be done by substituting z for ∇u allowing as to decouple the smooth L_2 term and the non-smooth regularization. It is then incorporated into the original objective using scaled augmented Lagrangian multiplier v, which leads to a joint minimization problem:

$$\min_{u,z} \frac{1}{2}||DHIWu - g||_2^2 + \frac{\rho}{2}||\nabla u - z + v||_2^2 + \gamma||z||_1 - \frac{\rho}{2}\|v\|_2^2$$

We can now minimize both terms separately. ADMM does this by repeating the following 3 steps in each iteration:

1. Updates u by solving

$$u = \arg\min_u \frac{1}{2}||DHIWu - g||_2^2 + \frac{\rho}{2}||\nabla u - z + v||_2^2$$

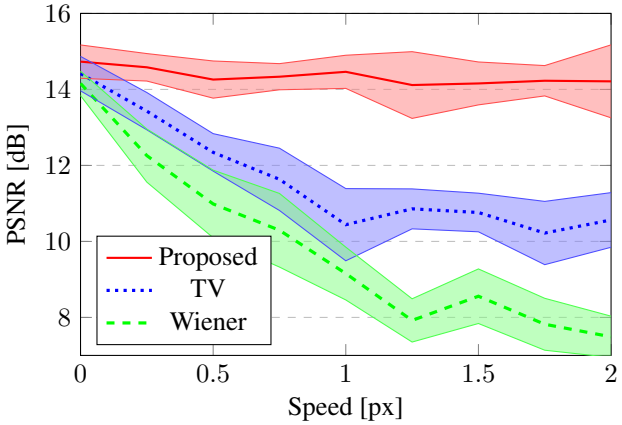

Fig. 2: Performance of the reconstruction algorithms on synthetic data with respect to the linear motion speed (in pixels per frame) of the simulated object.

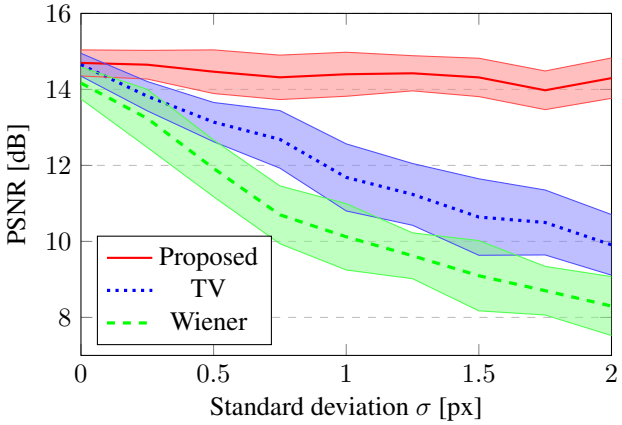

Fig. 3: Performance of the reconstruction algorithms on synthetic data with respect to the standard deviation of the Brownian motion (in pixels per frame) of the simulated object.

2. Updates z by solving

$$z = \arg\min_z \frac{\rho}{2}||\nabla u - z + v||_2^2 + \gamma||z||_1$$

3. Updates v by setting $v = v + \nabla u - z$

The first update does not have a closed form solution and must be solved iteratively. We are using the conjugate gradient (CG) method [16]. In practice, only a few CG iterations are sufficient for convergence.

The z update can be rearranged into a more suitable form:

$$z = \arg\min_z \frac{\gamma}{\rho}||z||_1 + \frac{1}{2}||z - (\nabla u + v)||_2^2$$

and solved independently per-pixel using a proximal operator [17]. The proximal operator of a scaled function $\lambda f(q)$ is defined as:

$$\text{prox}_{\lambda f}(q) = \arg\min_p f(p) + \frac{1}{2\lambda}||p - q||_2^2$$

By setting $f(z) = ||z||_1$, $\lambda = \frac{\gamma}{\rho}$ and $q = \nabla u + v$ we get the equivalent problem. Finally, the original minimization can be solved using the known closed form solution of the proximal operator:

$$\text{prox}_{\lambda||p||_1}(q) = \text{sign}(q)\max(0, |q| - \lambda)$$

There are three parameters in the algorithm above: the regularization weight γ, the acceleration ρ and the number of iterations. For the experiments in the next section, we use $\gamma = \rho = 1$ and 20 ADMM iterations.

2.4. Parameter estimation

The image formation operators H, I and W are parametrized, and their parameters have to be established before the optimization problem can be solved.

The convolution operator H requires the knowledge of the PSF. It can be measured experimentally or approximated using a mathematical model. In our case, we are approximating the OTF as the auto-correlation of the pupil function [10].

The illumination operator I depends on the properties of the structured illumination patterns. Generally, the system is not stable enough and the parameters have to be estimated from the observed images g. Extensive research deals with the issue of their estimation [18], even under difficult conditions [19], hence the specific methods will not be discussed here.

The warping operator W simulates the local inter-frame movement which is obviously not known. In our experiments, we calculate the motion estimation using dense optical flow. More specifically, we up-sample the original images g to the size of u using cubic interpolation, mildly blur them using a Gaussian and finally calculate the optical flow by a single-stage Farneback algorithm [20] with a small window.

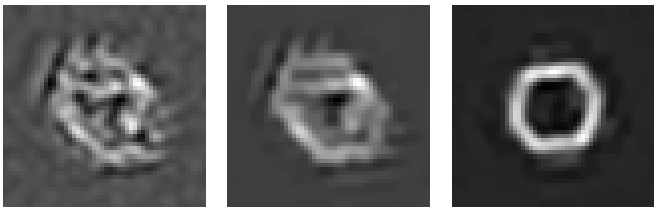

(a) Wiener (b) TV (c) Proposed

Fig. 4: Examples of reconstruction using different algorithms on synthetic data with linear motion from bottom right to top left with speed of 1 pixel per frame (See Fig. 2).

3. EXPERIMENTS

We demonstrate the performance of our method in several experiments with both synthetic and real live-cell microscopy

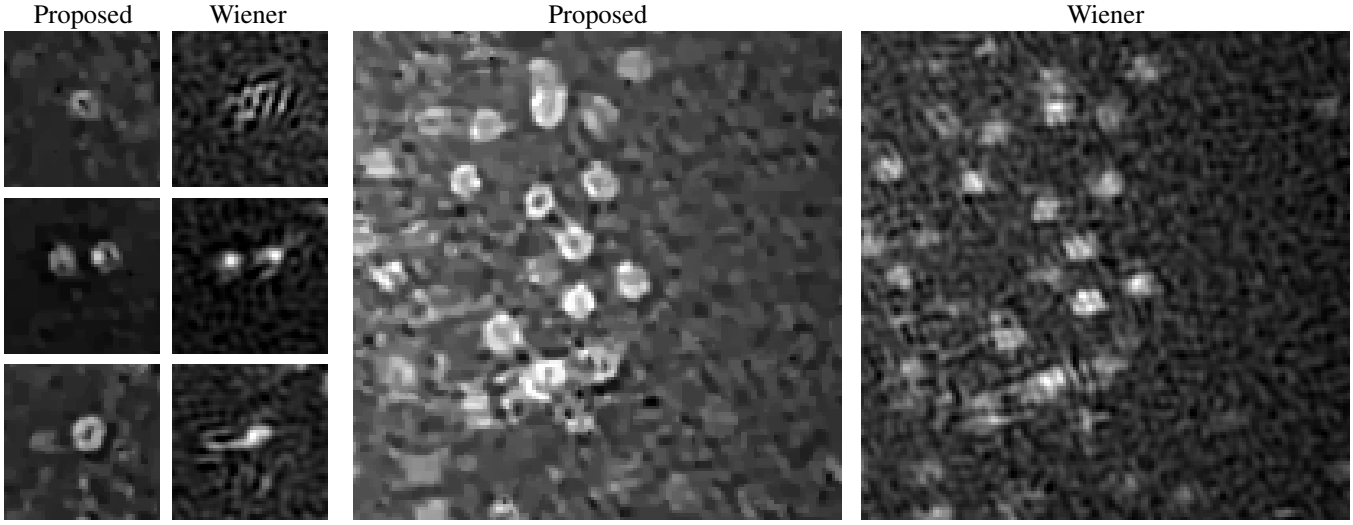

Fig. 5: Selected examples of reconstruction using the proposed approach and the traditional Wiener filtering on real biological data. The observed sub-cellular structures are known to have the shape of an annulus.

data. For comparison, we also show the results obtained with the traditional Wiener filtering approach [4] and an iterative optimization approach with TV regularization similar to the proposed approach, but without the movement compensation.

In the first experiment with synthetic data, we simulate the movement of a sub-cellular structure represented by a circle with a diameter of approximately 20 pixels. In the reference middle frame, the object is always exactly in the centre of the frame. In the preceding and subsequent frames, it moves either linearly or in a random Brownian motion, and the movement distance in each direction is sampled from the normal distribution. The base synthetic images are then illuminated with a known structured light pattern, convolved with a PSF, down-sampled and augmented with a random Poisson noise. Finally, the nine low-resolution images generated in this way were reconstructed by the different algorithms and we measured the resulting peak signal-to-noise ratio (PSNR) depending on the linear speed or standard deviation of the normal distribution, respectively. An example of the resulting reconstructions is shown in Fig. 4.

To achieve less ambiguity in our experiments, we performed the reconstruction multiple times for each parameter with different noise and motion orientation. Figs. 2 and 3 show both the mean values and their standard deviation. It is clear from the results that the proposed method is very robust to even large movement.

The second experiment in Fig. 5 illustrates the benefit of the proposed method on real live-cell microscopy images. For this purpose, we used a custom-built eTIRF-SIM to obtain data that captures the formation of endocytic vesicles at the membrane of an epithelial cell line [21]. The vesicles appear as small protein assemblies at the plasma membrane that gradually enlarge into rings in the exponentially decaying intensity of the incident light with the evanescent TIRF field. Each low-resolution frame was illuminated for approximately 60ms with the total time of six minutes resulting in around 60-120 high-resolution images. We have reconstructed the movies with both the Wiener reconstruction used with this setup previously and with the newly proposed method. From these we hand-selected representative smaller cut-outs that clearly demonstrate the differences between them.

It should be mentioned that although in most cases the proposed method achieved better results without reconstruction artifacts caused by the movement, there are still cases where the results are suboptimal and where the object identity and interpretation are obscure. This can be seen in parts of Fig. 5 (b).

4. CONCLUSION

We have proposed a direct extension to SIM image reconstruction suitable for fast super-resolution live-cell imaging. We established this extension in the image formation model forward problem with a simple TV regularization. Next, we derived the iterative solution of this optimization using ADMM. An optical flow algorithm was used to estimate the local motion. We have demonstrated the method's applicability on synthetic data and on data from a real microscope. A more detailed analysis of local movement estimation methods and different regularization techniques will be addressed in future work.

5. REFERENCES

[1] Ernst Abbe, "Beiträge zur theorie des mikroskops und der mikroskopischen wahrnehmung," *Archiv für mikroskopische Anatomie*, vol. 9, no. 1, pp. 413–468, 1873.

[2] Peyman Milanfar, *Super-resolution imaging*, CRC press, 2017.

[3] Stefan W Hell and Jan Wichmann, "Breaking the diffraction resolution limit by stimulated emission: stimulated-emission-depletion fluorescence microscopy," *Optics letters*, vol. 19, no. 11, pp. 780–782, 1994.

[4] Mats GL Gustafsson, "Surpassing the lateral resolution limit by a factor of two using structured illumination microscopy," *Journal of microscopy*, vol. 198, no. 2, pp. 82–87, 2000.

[5] Keith A Lidke, Bernd Rieger, Thomas M Jovin, and Rainer Heintzmann, "Superresolution by localization of quantum dots using blinking statistics," *Optics express*, vol. 13, no. 18, pp. 7052–7062, 2005.

[6] Daniel Axelrod, "Cell-substrate contacts illuminated by total internal reflection fluorescence.," *The Journal of cell biology*, vol. 89, no. 1, pp. 141–145, 1981.

[7] Reto Fiolka, Markus Beck, and Andreas Stemmer, "Structured illumination in total internal reflection fluorescence microscopy using a spatial light modulator," *Optics letters*, vol. 33, no. 14, pp. 1629–1631, 2008.

[8] Julian Roth, Johanna Mehl, and Alexander Rohrbach, "Fast tirf-sim imaging of dynamic, low-fluorescent biological samples," *Biomedical optics express*, vol. 11, no. 7, pp. 4008–4026, 2020.

[9] Ronny Förster, Walter Müller, René Richter, and Rainer Heintzmann, "Automated distinction of shearing and distortion artefacts in structured illumination microscopy," *Optics express*, vol. 26, no. 16, pp. 20680–20694, 2018.

[10] François Orieux, Eduardo Sepulveda, Vincent Loriette, Benoit Dubertret, and Jean-Christophe Olivo-Marin, "Bayesian estimation for optimized structured illumination microscopy," *IEEE Transactions on image processing*, vol. 21, no. 2, pp. 601–614, 2011.

[11] Jérôme Boulanger, Nelly Pustelnik, Laurent Condat, Lucie Sengmanivong, and Tristan Piolot, "Nonsmooth convex optimization for structured illumination microscopy image reconstruction," *Inverse problems*, vol. 34, no. 9, pp. 095004, 2018.

[12] Emeric Mudry, Kamal Belkebir, J Girard, Julien Savatier, Emmeran Le Moal, C Nicoletti, Marc Allain, and Anne Sentenac, "Structured illumination microscopy using unknown speckle patterns," *Nature Photonics*, vol. 6, no. 5, pp. 312–315, 2012.

[13] Li-Hao Yeh, Lei Tian, and Laura Waller, "Structured illumination microscopy with unknown patterns and a statistical prior," *Biomedical optics express*, vol. 8, no. 2, pp. 695–711, 2017.

[14] Leonid I Rudin, Stanley Osher, and Emad Fatemi, "Nonlinear total variation based noise removal algorithms," *Physica D: nonlinear phenomena*, vol. 60, no. 1-4, pp. 259–268, 1992.

[15] Stephen Boyd, Neal Parikh, and Eric Chu, *Distributed optimization and statistical learning via the alternating direction method of multipliers*, Now Publishers Inc, 2011.

[16] Magnus R Hestenes and Eduard Stiefel, "Methods of conjugate gradients for solving," *Journal of research of the National Bureau of Standards*, vol. 49, no. 6, pp. 409, 1952.

[17] Jean-Jacques Moreau, "Proximité et dualité dans un espace hilbertien," *Bulletin de la Société mathématique de France*, vol. 93, pp. 273–299, 1965.

[18] Marcel Lahrberg, Mandeep Singh, Kedar Khare, and Balpreet Singh Ahluwalia, "Accurate estimation of the illumination pattern's orientation and wavelength in sinusoidal structured illumination microscopy," *Applied optics*, vol. 57, no. 5, pp. 1019–1025, 2018.

[19] Kaiqin Chu, Paul J McMillan, Zachary J Smith, Jie Yin, Jeniffer Atkins, Paul Goodwin, Sebastian Wachsmann-Hogiu, and Stephen Lane, "Image reconstruction for structured-illumination microscopy with low signal level," *Optics express*, vol. 22, no. 7, pp. 8687–8702, 2014.

[20] Gunnar Farnebäck, "Two-frame motion estimation based on polynomial expansion," in *Scandinavian conference on Image analysis*. Springer, 2003, pp. 363–370.

[21] Nathan R Zaccai, Zuzana Kadlecova, Veronica Kane Dickson, Kseniya Korobchevskaya, Jan Kamenicky, Oleksiy Kovtun, Perunthottathu K Umasankar, Antoni G Wrobel, Jonathan GG Kaufman, Sally R Gray, et al., "Fcho controls ap2's initiating role in endocytosis through a ptdins (4, 5) p2-dependent switch," *Science advances*, vol. 8, no. 17, pp. eabn2018, 2022.